An Adaptive Hysteresis Band Controller for *LC*-coupling Hybrid Active Power Filter with Approximate Constant Switching Frequency

Lei Wang[1], Chi-Seng Lam[1,2] and Man-Chung Wong[1,2]

1 - Department of Electrical and Computer Engineering, Faculty of Science and Technology, University of Macau,
2 - State Key Laboratory of Analog and Mixed-Signal VLSI, University of Macau,
Macau, China
yb27422@umac.mo/C.S.Lam@ieee.org

***Abstract*—This paper presents an adaptive hysteresis band controller for *LC*-coupling hybrid active power filter (HAPF) which can provide an approximate constant switching frequency. As the *LC*-coupling impendence can yield nonlinear compensating current slope, the conventional adaptive hysteresis band controller for linear *L*-coupling system like active power filter (APF) cannot be directly applied to nonlinear *LC*-coupling HAPF system. Owing to the circuit configuration of HAPF, its compensating current characteristic is firstly analyzed and discussed. The adaptive hysteresis band current controller for HAPF is then proposed by considering its nonlinear characteristic. Finally, to verify the performance of the proposed adaptive hysteresis band controller, simulation results are given in comparison with both conventional adaptive hysteresis band controller (developed for *L*-coupling system) and fixed hysteresis band controller for HAPF.**

***Index Terms*--Power quality, pulse width modulation, power filters, switching frequency.**

I. INTRODUCTION

Power system filters are the solutions for the power quality problems such as low power factor, harmonic pollution, and large power loss. Passive power filters (PPFs) are first installed in mid-1940 to address above problems. It cannot be dynamically adjusted with loading variation, as a result they may cause system resonance between the filter and the loading. On the other hand, the active power filters (APFs) can be employed to compensate the harmonic components and the reactive power dynamically. However, it requires higher dc-link voltage so that the system rating and the cost are higher. Nevertheless, a *LC*-coupling hybrid active power filter (HAPF) is a combination of a passive filter and an active filter, which can reduce the system rating and the initial cost of the compensator [1]-[7]. This structure is first proposed in [1] by Srianthumrong and Akagi in 2003. The authors use indirect current control (multiplying the reference current by a gain) in [1] to calculate the voltage reference. This indirect current pulse-width modulation (PWM) control method is sensitive to environmental factors and introduces errors into the reference signals. To enhance the HAPF system response, a novel control technique with ramp comparison PWM method (direct current control) [2] has also been proposed in 2009. However, there exist inherit magnitude and phase errors of the generated compensating current compared with its reference. Recently, current hysteresis PWM strategies (direct current control) are getting more popular due to their advantages: fast dynamic response, current error limiting capability and easy implementation, etc [3]-[15]. In 2012, the hysteresis PWM study of HAPF system is proposed in [3], which is the first publication to study the non-linear, quasi-linear and linear characteristics of the injected current in *LC*-coupling HAPFs. It is suggested to reduce the hysteresis band to be a small value based on 5% of the injected current slope, so that the compensating current can be linearized. However, this hysteresis band controller yields irregular switching frequency. Therefore, the current harmonics are not limited at one harmonic order, and more harmonic orders are generated.

To address above problems, adaptive hysteresis band controller methods have been recommended in literatures [8]-[15], in which adaptive hysteresis PWMs were extended into multi-level inverter applications [8] in 2012. For the adaptive hysteresis band controller, it can provide an approximate constant switching frequency and force the output harmonics at one dominant harmonic order, so that it is easier to further design a passive LC filter to mitigate the current harmonics. Unfortunately, the existing adaptive hysteresis band controllers were developed based on linear concept, which are usually applied to linear *L*-coupling systems such as APFs, dynamic voltage restorers (DVRs), ac motor drivers, etc. If the above adaptive hysteresis band controllers are directly applied to *LC*-coupling system like HAPF, the HAPF cannot operate at its designed fixed switching frequency due to its non-linear slope caused by coupling *LC*. In this paper, considering the nonlinearity of HAPF, an adaptive hysteresis band controller is designed, which can provide an approximate constant switching frequency.

978-1-4799-7537-2/14/$31.00 ©2014 IEEE

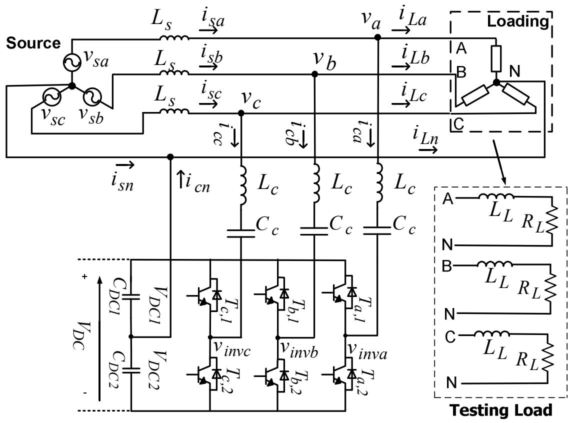

Figure 1. Circuit configuration of a three-phase four-wire HAPF

In this paper, the circuit configuration of HAPF will be firstly provided. Via its circuit configuration, the compensating current equation of HAPF will be deduced. Following that, the adaptive hysteresis band controller for HAPF will be proposed. Finally, simulation results of the proposed adaptive hysteresis band controller are presented in comparison to both conventional adaptive hysteresis band controller (developed for *L*-coupling system) [12] and the fixed hysteresis band controller for HAPF.

II. Circuit Configuration of a Three-phase Four-wire Center-split HAPF

The circuit configuration of the three-phase four-wire center-split HAPF is shown in Fig. 1. For the following analysis, the subscript '*x*' denotes phase *x* = *a, b, c* and *n*. v_{sx} is the system voltage, v_x is the terminal load voltage, L_s is the system inductor, L_c is the coupling inductor and C_c is the coupling capacitor. i_{sx}, i_{Lx} and i_{cx} are the source, load and compensating currents respectively. v_{invx} is the inverter voltage. C_{DC1} and C_{DC2} are upper and lower dc-link capacitors, while V_{DC1} and V_{DC2} are upper and lower dc-link voltages. V_{DC} is the total dc-link voltage which is the sum of V_{DC1} and V_{DC2}. Via this circuit configuration, the compensating current i_{cx} of HAPF will be deduced and discussed as follows.

III. Compensating Current Characteristics of HAPF

Under the HAPF compensation, the switching state of an inverter leg is independent of the switching states of the other two legs. According to Fig. 1, the mathematical modeling of HAPF can be deduced:

$$L_c \frac{di_{cx}(t)}{dt} + \frac{1}{C_c}\int i_{cx}(t)dt = v_x(t) - v_{invx}(t) \tag{1}$$

Taking the derivative of (1), it yields:

$$L_c \frac{d^2 i_{cx}(t)}{dt^2} + \frac{1}{C_c} i_{cx}(t) = \frac{d[v_x(t) - v_{invx}(t)]}{dt} \tag{2}$$

where i_{cx} is the compensating current, L_c is coupling inductor, C_c is coupling capacitor and $v_{invx}(t)$ is inverter voltage. It can be clearly observed that (2) is a second order equation in term of $i_{cx}(t)$.

Take the Laplace transform of (2) and simplify it. After that, substitute initial compensating current and capacitor voltage conditions into the characteristic Laplace equation. Finally, the time domain $i_{cx}(t)$ solution (3) can be obtained by taking inverse Laplace transformation as:

$$i_{cx}(t) = A \cdot sin(\omega_0 t + \phi) \tag{3}$$

where

$$A(t) = \sqrt{i_{cx}^2(0) + \frac{C_c}{L_c} \cdot [v_x(t) - v_{invx}(t) - v_{C_c}(0)]^2} \tag{4}$$

$$\omega_0 = \frac{1}{\sqrt{L_c \cdot C_c}} \tag{5}$$

$$\phi = tan^{-1}\left(\frac{\sqrt{L_c}}{\sqrt{C_c}} \cdot \frac{i_{cx}(0)}{v_x(t) - v_{invx}(t) - v_{C_c}(0)} \right) \tag{6}$$

The compensating current $i_{cx}(t)$ is expressed in terms of coupling inductor L_c, coupling capacitor C_c, initial compensating current $i_{cx}(0)$, initial capacitor voltage $v_{C_c}(0)$, load voltage $v_x(t)$ and inverter voltage $v_{invx}(t)$, where the value of $v_{invx}(t)$ can be obtained from dc-link voltage V_{DC} and switching states. Via (3)-(6), the adaptive hysteresis band current controller for HAPF will be investigated and proposed in the following section.

IV. Adaptive Hysteresis Band Current Controller for HAPF

In this section, the adaptive hysteresis band current controller for HAPF is investigated in compared with conventional adaptive hysteresis band controller. Firstly, the conventional adaptive hysteresis band for *L*-coupling system will be briefly introduced and compared. Then, the relationship between hysteresis band and the amplitude of compensating current is discussed. Finally, the adaptive hysteresis band controller is proposed to provide an approximate constant switching frequency for HAPF system.

A. Conventional adaptive hysteresis band for L-coupling system

The conventional adaptive hysteresis band was developed based on linear concept, which is usually applied on *L*-

coupling systems such as APF, DVR, ac motor drivers etc. The time based hysteresis band can be expressed as [12]:

$$H(t)=\frac{V_{DC}}{8L_c f_{sw}}\left[1-\frac{4L_c^2}{V_{DC}^2}\left(\frac{v_x(t)}{L_c}-\frac{di_{cx}^*(t)}{dt}\right)^2\right] \quad (7)$$

where $v_x(t)$ is the instantaneous load voltage, V_{DC} is the dc-link voltage, f_{sw} is the switching frequency, L_c is the coupling inductor and $i_{cx}^*(t)$ is the reference compensating current.

As the L-coupling systems do not contain coupling capacitor, therefore, if the conventional adaptive hysteresis band controller (7) is directly applied to HAPF system, the nonlinearity of the compensating current due to its coupling LC part can deteriorate HAPF controllability. Moreover, because the dc-link voltage is normally lower than load voltage for HAPF, a negative hysteresis band value will be obtained through (7). In order to obtain an approximate constant switching frequency for HAPF, the adaptive hysteresis band controller is necessary to develop for HAPF, which will be proposed in the following two parts.

B. Relationship between hysteresis band and compensating current

Fig. 2 illustrates the relationship between the amplitude of compensating current and hysteresis band. If the hysteresis band is set to be larger than the amplitude of compensating current ($H(t)>A(t)$), no trigger signal will be generated as shown in Fig. 2(a). If the hysteresis band is set to be equal to the amplitude of compensating current ($H(t)=A(t)$) as shown in Fig. 2(b), the lowest switching frequency can be obtained. Moreover, if the hysteresis band is set to be α times ($\alpha<1$) smaller than the amplitude of compensating current ($H(t)=\alpha\cdot A(t)<A(t)$), the hysteresis band can be strictly limited under the hysteresis band as shown in Fig. 2(c). Based on the characteristics of the compensation current as shown in (3) and Fig. 2(b), the lowest switching frequency of the HAPF can obtained as:

$$f_{sw\_lowest}=\frac{1}{2\pi\cdot\sqrt{L_cC_c}} \quad (8)$$

In (8), it can be seen that f_{sw_lowest} depends the passive part (L_c and C_c) values. On the other hand, the theoretical fastest switching frequency $f_{sw\_fastest}$ depends on the fasting sampling frequency by AD converter. Therefore, the final switching frequency range that controlled by hysteresis band is $f_{sw}\in[\,f_{sw\_lowest}\quad f_{sw\_fastest}\,]$.

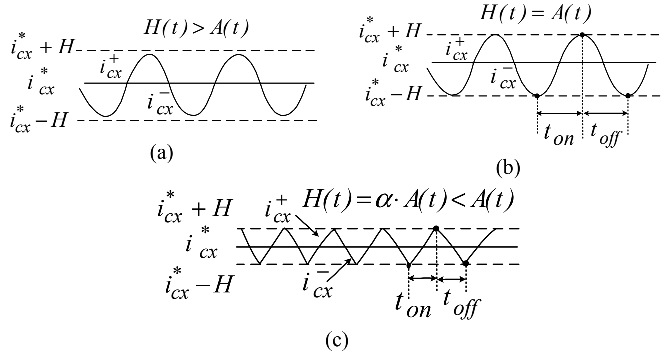

Figure 2. Hysteresis band discussions under constant reference current (a) $H(t)>A(t)$ (b) $H(t)=A(t)$ (c) $H(t)=\alpha\cdot A(t)<A(t)$

Based on above discussions of relationship between $H(t)$ and $A(t)$, the adaptive hysteresis band controller will be proposed to provide an approximate constant switching frequency under the situation of $H(t)\le A(t)$.

C. Proposed Adaptive Hysteresis Band Controller

Fig. 3 describes the idea of the proposed adaptive hysteresis band for HAPF. From the geometry of Fig. 3, the following equations can be obtained.

$$2\cdot H(t_1)=2\cdot\alpha\cdot A(t_1)-\frac{di_{cx}^*}{dt}t_{on} \quad (9)$$

$$2\cdot H(t_2)=2\cdot\alpha\cdot A(t_2)+\frac{di_{cx}^*}{dt}t_{off} \quad (10)$$

$$2\cdot H(t_3)=2\cdot\alpha\cdot A(t_3)-\frac{di_{cx}^*}{dt}t_{on} \quad (11)$$

where $H(t)$ is the instantaneous hysteresis band and $A(t)$ is the amplitude of the compensating current from (4). Combining (9), (10) and (11), then substituting $f_{sw}=1/(t_{on}+t_{off})$ into them, the instantaneous hysteresis band can be obtained as:

$$H(t_2)=\alpha\cdot A(t_2)+[H(t_1)-\alpha\cdot A(t_1)]+\frac{1}{2f_{sw}}\frac{di_{cx}^*(t)}{dt} \quad (12)$$

$$H(t_3)=\alpha\cdot A(t_3)+[H(t_2)-\alpha\cdot A(t_2)]-\frac{1}{2f_{sw}}\frac{di_{cx}^*(t)}{dt} \quad (13)$$

In the steady state, the scale factor α is a constant value. So the general form of adaptive hysteresis band can be summarized as:

$$H(t_n)=\alpha\cdot A(t_n)+[H(t_{n-1})-\alpha\cdot A(t_{n-1})]-\frac{S_x}{2f_{sw}}\frac{di_{cx}^*(t)}{dt} \quad (14)$$

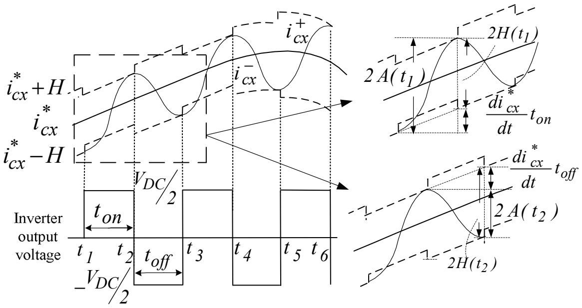

Figure 3. The idea of proposed adaptive hysteresis band controller for controlling of compensating current

where $A(t_n)$ and $A(t_{n-1})$ are amplitude of i_{cx} from (4) in the current state and previous state respectively, $H(t_n)$ and $H(t_{n-1})$ are output hysteresis band of current state and previous state, f_{sw} is the switching frequency and S_x is the switching state. S_x is equal to *1* when upper IGBT $T_{x,1}$ is on and lower IGBT $T_{x,2}$ is off, otherwise S_x is equal to *-1*.

Practically, the term $\alpha \cdot A(t_n)$ is dominant in (14). The term $A(t_{n-1}) - \alpha \cdot A(t_{n-1})$ is equal to $-\frac{t_{on}}{2}\frac{di_{cx}^{*}}{dt}$ for $S_x = -1$, and it is equal to $\frac{t_{off}}{2}\frac{di_{cx}^{*}}{dt}$ for $S_x = 1$. In order to simplify (14), the term $A(t_{n-1}) - \alpha \cdot A(t_{n-1})$ can be approximated equal to $\frac{S_x}{4f_{sw}}\frac{di_{cx}^{*}}{dt}$. Therefore, the simplified version of (14) can be obtained as:

$$H(t_n) = \alpha \cdot A(t_n) - \frac{S_x}{4f_{sw}}\frac{di_{cx}^{*}(t)}{dt} \tag{15}$$

Comparing (14) with (15), (14) gives more accurate constant switching frequency hysteresis band control equation for HAPF. However, (15) has less calculating cycles and is easier to implement in to digital controller. And (15) gives the idea that hysteresis band $H(t)$ can be changed adequately to keep switching frequency f_{sw} at the desired constant value. The scale factor α can be determined by comparing the detected average f_{sw} with the target f_{sw}^{*} though a PI controller. If the detected average f_{sw} is equal to target f_{sw}^{*}, the corresponding α can be selected. Otherwise, the value of α is modified with the PI gain signal. And the scale factor α is a fixed value in the steady state.

Based on the passive part (L_c and C_c) components values and the inputs signals v_x, v_{C_c}, V_{DC}, i_{cx}, the compensating current $A(t)$ can be obtained though (4). With α, target f_{sw}^{*}, $A(t)$ and S_x, the adaptive hysteresis band $H(t)$ can be calculated through (15) to generate switching trigger signals.

In the following, the simulation results of the proposed controller (15) will be provided in comparison with both conventional adaptive hysteresis band controller (developed for *L*-coupling system) via (7) and fixed hysteresis band controller for HAPF.

V. SIMULATION RESULTS

The simulation results of proposed adaptive hysteresis band controller for HAPF are presented in comparison with results of both conventional adaptive hysteresis band controller (developed for *L*-coupling system) [12] and fixed hysteresis band controller for HAPF. Simulation studies were carried out by using PSCAD/EMTDC. And the system parameters, HAPF parameters and testing load are provided in Table I. The target switching frequency f_{sw}^{*} is set to be 1kHz for both conventional adaptive hysteresis band controller and proposed controller. Fig. 4 gives the simulation results of compensating current, compensated source current total harmonic distortion (THD_i) and compensated source current spectrum by applying different controllers. Table II summarizes their corresponding simulation results before and after compensation.

TABLE I. PARAMETERS OF SYSTEM, HAPF AND TESTING LOAD

	Parameters	Physical values
System parameters	v_x, f, L_s	$110V$, $50Hz$, $0.5mH$
HAPF parameters	L_c, C_c	$5mH$, $140\mu F$
	C_{DC1}, C_{DC2}	$5mF$, $5mF$
	V_{DC1}, V_{DC2}	$30V$, $30V$
Testing load	L_L, R_L	$30mH$, 12Ω

From Fig. 4(a), the compensating current is not sinusoidal waveform for linear testing load when the conventional adaptive hysteresis controller (developed for *L*-coupling system) is directly applied to HAPF. The harmonics are large at low orders as shown in Fig. 4(d). From Table II, it can be seen that THD_i is 20.1%, which cannot satisfy the international standards [16], [17]. Besides, the switching frequency has the large variation from 0.01k Hz to17.05kHz as shown in Table. II, and it cannot trace the target f_{sw}^{*}. Therefore, the adaptive hysteresis band controller (developed for *L*-coupling system) cannot be directly applied to HAPF system. For fixed hysteresis band controller, the switching frequency is varying from 0.45kHz to 1.67kHz as shown in Table. II. In Fig. 4(e), it can be observed that the harmonic currents are distributed at all harmonic frequencies. So, it is difficult to design suitable filters to mitigate all these harmonic currents. For the proposed adaptive hysteresis band controller, the switching frequency has the small variation and it can approximately trace the target f_{sw}^{*} as shown in Table. II. Besides, the source current harmonics are small except around the dominant harmonic order. Therefore, it is easier to design a passive LC filter to eliminate the corresponding dominant current harmonics. The validity of proposed adaptive hysteresis band controller is proved by simulation results in Fig. 4 and Table II.

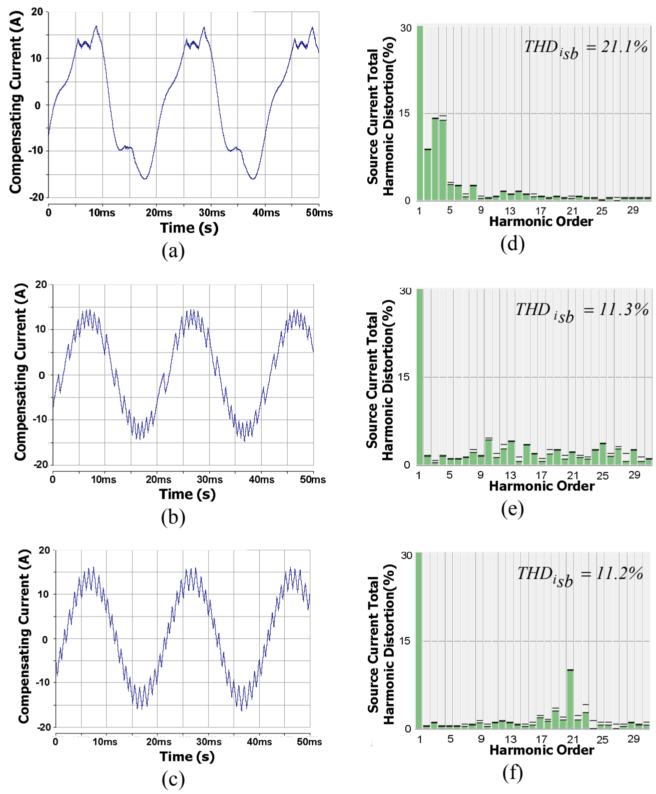

Figure 4. Simulation waveform of i_{cx} by using (a) conventional adaptive hysteresis band controller (developed for *L*-coupling system), (b) fixed hysteresis band controller and (c) proposed adaptive hystereis band controller. Source current spectrum after compensation by (d) adaptive hysteresis band (developed for *L*-coupling system), (e) fixed hysteresis band controller and (f) proposed adaptive hystereis band controller.

TABLE II. SIMULATED RESULTS BY USING ADAPTIVE HYSTERESIS BAND CONTROLLER (DEVELOPED FOR *L*-COUPLING SYSTEM), FIX HYSTERESIS BAND CONTROLLER AND PROPOSED ADAPTIVE HYSTERESIS BAND CONTROLLER BEFORE AND AFTER COMPENSATION

	Before HAPF compensation	Conventional method [12]	Fix band method	Proposed method
i_{sx} (A)	14.22	11.63	11.56	11.44
i_{sn} (A)	0.02	5.45	2.06	1.75
DPF (%)	0.78	0.99	1.00	1.00
THD_i (%)	0.48	20.1	11.3	11.2
$f_{sw(max)}$ (Hz)	--	17.05 k	1.67 k	1.20 k
$f_{sw(min)}$ (Hz)	--	0.01 k	0.45 k	0.91 k

VI. CONCLUSION

In this paper, an adaptive hysteresis band controller for HAPF with an approximate constant switching frequency is investigated and discussed. On the basis of the circuit configuration of HAPF, the nonlinear characteristic of its compensating current is discussed mathematically. With considering its nonlinear characteristic, the adaptive hysteresis band controller for HAPF is investigated to provide an approximate constant switching frequency. Finally, the simulation results of the proposed adaptive HAPF hysteresis band controller are presented in comparison with results of both adaptive hysteresis band controller (developed for *L*-coupling system) [12] and fix hysteresis band controller for HAPF. By applying the proposed adaptive HAPF hysteresis band controller, approximate constant switching frequency is achieved.

References

[1] S. Srianthumrong and H. Akagi, "A medium-voltage transformerless AC/DC Power conversion system consisting of a diode rectifier and a shunt hybrid filter," *IEEE Trans. Ind. Appl.,* vol. 39, pp. 874 – 882, May/Jun. 2003.

[2] S. Rahmani, A. Hamadi, N. Mendalek and K. Al-Haddad, "A new control technique for three-phase shunt hybrid power filter," *IEEE Trans. Ind. Electron.,* vol. 56, no. 8, pp. 2904 – 2915, Aug. 2009.

[3] C. S. Lam, M. C. Wong and Y. D. Han, "Hysteresis current control of hybrid active power filters," *IET Power Electron.,* vol.5, no. 7, 1175-1187, Aug. 2012.

[4] Chi-Seng Lam, Man-Chung Wong, Wai-Hei Choi, Xiao-Xi Cui, Hong-Ming Mei, Jian-Zheng Liu, "Design and performance of an adaptive low dc voltage controlled LC-hybrid active power filter with a neutral inductor in three-phase four-wire power systems", *IEEE Trans. Ind. Electron,* vol. 61, no, 6, pp. 2635 □ 2647, Jun. 2014.

[5] Chi-Seng Lam, Wai-Hei Choi, Man-Chung Wong, Ying-Duo Han, "Adaptive dc-link voltage controlled hybrid active power filters for reactive power compensation", *IEEE Trans. Power Electron.,* vol. 27, no, 4, pp. 1758 - 1772,Apr. 2012.

[6] Wai-Hei Choi, Chi-Seng Lam, Man-Chung Wong, Ying-Duo Han, "Analysis of dc-link voltage controls in three-phase four-wire hybrid active power filters", *IEEE Trans. Power Electron.,* vol. 28, no, 5, pp. 2180 - 2191,May 2013.

[7] Chi-Seng Lam, Xiao-Xi Cui, Wai-Hei Choi, Man-Chung Wong, Ying-Duo Han, "Minimum inverter capacity design for three-phase four-wire LC-hybrid active power filters", *IET Power Electron.,* vol. 5, no. 7, pp. 956 - 968,Aug. 2012.

[8] H. Mao, X. Yang, Z. Chen, and Z. Wang, "A Hysteresis Current Controller for Single-Phase Three-Level Voltage Source Inverters," *IEEE Trans. Power Electron.*, vol.27, no.7, pp.3330-3339, July 2012

[9] D. G. Holmes, R. Davoodnezhad and B. P. McGrath "An Improved Three-Phase Variable-Band Hysteresis Current Regulator," *IEEE Trans. Power Electron.*, vol.28, no.1, pp.441-450, Jan. 2013.

[10] Q. Yao and D. G. Holmes, "A simple, novel method for adaptive-hysteresis-band current control of a three phase inverter with constant switching frequency," *Conf. Rec. IEEE-IAS Annu Meeting.,* vol. 2, pp. 1122–1129. Oct. 1993.

[11] T. W. Chun and M. K. Choi, "Development of adaptive hysteresis band control strategy of PWM inverter with constant switching frequency," *Proc. IEEE APEC'96,* vol. 1, pp. 194–199. Mar. 1996.

[12] B. J Kang, "A robust hysteresis current-controlled PWM inverter for linear PMSM driven magnetic suspended positioning system," *IEEE Trans. Ind. Applicat.,* vol. 48, no. 5 pp: 956 – 967, Oct 2001.

[13] B. K. Bose, "An adaptive hysteresis-band current control technique of a voltage-fed PWM inverter for machine drive system," *IEEE Trans. Ind. Applicat.,* vol. 37, no. 5, pp. 402– 408, Oct.1990.

[14] L. Malesani, P. Mattavelli, and P. Tomasin, "Improved constant-frequency hysteresis current control of VSI inverters with simple feed forward bandwidth prediction," *IEEE Trans. Ind. Appl.,* vol. 33, no. 5, pp. 1194–1202, Sep./Oct. 1997.

[15] K. M. Rahman, M. R. Khan, M. A. Choudhury, and M. A. Rahman, "Variable-band hysteresis current controllers for PWM voltage-source inverters," *IEEE Trans. Power Electron.,* vol. 12, no. 6, pp. 964–970, Nov. 1997.

[16] *IEEE Recommended Practices and Requirements for Harmonic Control in Electrical Power Systems,* IEEE Std. 519-1992, Apr. 1993.

[17] *Electromagnetic Compatibility (EMC), Part 3: Limits, Section 2: Limits for Harmonics Current Emissions (Equipment Input Current <16A Per Phase),* IEC Standard 61000-3-2, 1997.